

Volume distribution for particles between 3.5 to 2000 μm in the upper 200 m region of the South Pacific Gyre

L. Stemmann^{1,2}, D. Eloire³, A. Sciandra¹, G. A. Jackson⁴, L. Guidi^{1,2}, M. Picheral¹, and G. Gorsky¹

¹Laboratoire d'Océanographie de Villefranche (LOV), Observatoire Océanologique, BP 28, 06234 Villefranche sur mer Cedex, France

²Université Pierre et Marie Curie-Paris6, UMR 7093, Villefranche sur Mer, 06234 France, Laboratoire d'Océanographie de Villefranche (LOV), Observatoire Océanologique, BP 28, 06234 Villefranche sur mer Cedex, France

³Plymouth Marine Laboratory, Prospect Place, Plymouth, PL1 3DH, UK

⁴Department of Oceanography, Texas A&M University, College Station, TX 77843, USA

Received: 12 September 2007 – Published in Biogeosciences Discuss.: 27 September 2007

Revised: 3 January 2008 – Accepted: 1 February 2008 – Published: 3 March 2008

Abstract. The French JGOFS BIOSOPE cruise crossed the South Pacific Gyre (SPG) on a transect between the Marquesas Islands and the Chilean coast on a 7500 km transect (8°S – 34°S and 8°W – 72°W). The number and volume distributions of small ($3.5 < d < 30 \mu\text{m}$) and large particles ($d > 100 \mu\text{m}$) were analysed combining two instruments, the HIAC/Royco Counter (for the small particles) and the Underwater Video Profiler (UVP, for the large particles). For the HIAC analysis, samples were collected from 12 L CTD Rosette bottles and immediately analysed on board while the UVP provided an estimate of in situ particle concentrations and size in a continuous profile. Out of 76 continuous UVP and 117 discrete HIAC vertical profiles, 25 had both sets of measurements, mostly at a site close to the Marquesas Islands (site MAR) and one in the center of the gyre (site GYR). At GYR, the particle number spectra from few μm to few mm were fit with power relationships having slopes close to -4 . At MAR, the high abundance of large objects, probably living organisms, created a shift in the full size spectra of particles such that a single slope was not appropriate. The small particle pool at both sites showed a diel pattern while the large did not, implying that the movement of mass toward the large particles does not take place at daily scale in the SPG area. Despite the relatively simple nature of the number spectra, the volume spectra were more variable because what were small deviations from the straight line in a log-log plot were large variations in the volume estimates. In addition, the mass estimates from the size spectra are very sensitive to crucial parameters such as the fractal dimension and the POC/Dry Weight ratio. Using consistent values for

these parameters, we show that the volume of large particles can equal the volume of the smaller particles. However the proportion of material in large particles decreased from the mesotrophic conditions at the border of the SPG to the ultra-oligotrophy of the center in the upper 200 m depth. We expect large particles to play a major role in the trophic interaction in the upper waters of the South Pacific Gyre.

1 Introduction

The size distribution of particles is a fundamental property of marine systems, affecting ecological trophic interactions, the vertical transmission of solar energy and the downward transport of organic matter. Despite its fundamental importance, size distribution is difficult to measure because particles occur over a large range of size and composition, from sub-micrometer compact particles to large, cm-sized loose aggregates. Accurate characterization of the entire size distribution requires instruments with resolution fine enough to characterize the small particles but sampling volumes large enough to capture the large, rare aggregates. Such observations of large aggregates must be made in situ because due to their fragile structures they are easily disrupted when retrieved for shipboard observation. Until recently, only the retrieval and analysis of the smallest size fraction ($d < 100 \mu\text{m}$) was feasible. The lack of technology hindered the detection and sizing of larger aggregates. However, recent development of optic and in situ imaging technologies makes the measurement of the complete particle size spectra more rapid. The datasets produced by these instruments could be used in biogeochemical studies to assess particle biomasses and fluxes.



Correspondence to: L. Stemmann
(stemmann@obs-vlfr.fr)

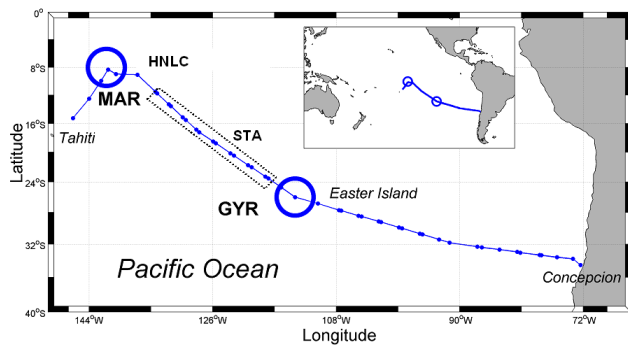


Fig. 1. Position of the short and long (large circle) stations during the BIOSOPE cruise.

Previous understanding was that the logarithm of particle concentration (expressed as a number spectrum) decreases almost proportionate to the logarithm of the particle diameter (d) with a slope of approximately 4 (Sheldon et al., 1972). Using this result, many authors have argued that there were equal volumes of living and non living particles in equal logarithmic size intervals for animals as large as the Loch Ness monster (Sheldon and Kerr, 1972). More recent analyses of a number spectra have combined different in situ instruments based on aperture impedance, imaging and optics (Jackson et al., 1995; Jackson et al., 1997; Mikkelsen et al., 2004). These observations of algal and detritic particles in both coastal waters and estuaries have challenged the above hypothesis. They show that most of the mass is found in aggregates larger than 100 μm and smaller than a few millimetres. To our knowledge, no particle size spectra for the range few μm to cm is yet available across surface oceans gyres.

The aims of the present study are to assess the vertical and temporal variability of the number and mass distributions of small ($3.5 < d < 30 \mu\text{m}$) and large particles ($d > 100 \mu\text{m}$) in the South Pacific Ocean. To do this, we analyse particle data from the French JGOFS BIOSOPE cruise that took place across the South Pacific Gyre (SPG). The size spectra of particles ranging from few μm to several mm were calculated from data collected using a HIAC/Royco Counter and the Underwater Video Profiler (Gorsky et al., 2000). With the observations, we were able to assess the contributions of both size fractions to the total biomass in different trophic conditions from the hyper-oligotrophic waters of the central gyre to the mesotrophic conditions of the Marquesas archipelago. In particular, we show the sensibility of the particle biomass assessment to the hypothesis made on the value of their porosity. The finding suggests that particle properties must be known before intensively using particle size spectra to assess biomass in biogeochemical studies.

2 Methods

2.1 Sampling sites

The French JGOFS BIOSOPE cruise sampled waters on a transect between the Marquesas Islands and the Chilean coast on a 7500 km transect (8°S – 34°S and 8°W – 72°W). The cruise was divided into two legs: Marquesas Archipelago (141°W , 8°S) to Easter Island (141°W , 26°S) and Easter Island to Concepcion, Chile (73°W , 35°S). Short duration stations (4 h, noted as STA for Leg 1 in Fig. 1) were located every 500 km and included measurement of biogeochemical and optical properties made by using 0–500 m vertical profiles of CTD-Rosette, optical devices, plankton nets. Three long duration stations during Leg 1 (4–5 days, noted as MAR, HNLC, GYR in Fig. 1) were located to sample contrasting systems more intensively by also using in situ pumps and sediment traps to collect particulate material. The particle size spectra from few μm to few mm were determined by combining data from a HIAC/Royco Counter and the Underwater Video Profiler (UVP). 76 UVP continuous casts during both Leg and 117 vertical discrete profiles for the HIAC (only during Leg 1) were performed. There were 25 UVP and HIAC combined profiles for Leg 1 and 15 combined profiles around the Marquesas Archipelago (MAR) and in the centre of the gyre near Easter Island (GYR). The profiles presented here are predominantly from MAR and GYR because of the additional information available from the time series measurements made there. Additional profiles are from the intermediate stations (5 profiles at HNLC, and 5 profiles at STA). MAR and GYR were chosen because they had the greatest difference in phytoplankton community structure and optical properties (Ras et al., 2007). The complete series of the UVP data from the upper 1000 m depth along the entire 8000 km transect are presented in (Guidi et al., 2008).

2.2 Particle-sizing instruments

Diameters d for particles $1.7 < d < 100 \mu\text{m}$ were determined on the ship using a HIAC/Royco particle counter (Pacific Scientific). The sensor's optical system (HRLD 400 HC) of the Hiac Counter (Model 3001) utilizes the principle of light-extinction for particle detection. The liquid sample flows through a sensor microcell where a laser beam is directed through a window at the sample. The light intensity is sensed by the light-extinction photodiode and used for automatic and continuous gain control of the sensor. When a particle is present within the sensor microcell, the particle blocks the laser beam from the photodetector. These pulses are proportional in amplitude to the light intensity of light extinction which is a measure of the particle size. The instrument reports the size as Equivalent Spherical Diameter (ESD). Size calibration is performed with latex beads of known size, but whose refractive index is greater than the refractive index of marine particles. Samples were collected from 12 L CTD

Rosette bottles and immediately analysed on board. The incidence of sample handling (rosette sampling in the water column, and sampling in the rosette) on the size spectra is difficult to evaluate. Because the total processing by the HIAC counter took approximately two hours for a 24 bottles rosette cast, the HIAC was placed on a rotating table to prevent particles falling to the bottom of sample bottles. Despite this, control tests showed that the concentration measured on the same seawater sample split among the 24 bottles of the device decreased by about 20%, presumably due to particle aggregation and/or dissolution during the counting. Surprisingly, this trend was not accompanied by a significant change of the particle size spectra slopes. The sequence of analysis always proceeded from shallowest to deepest samples, so that the measurements were systematically more biased for the latter. We have also examined the merging of Coulter and Hiac available size spectra in the size range where the two devices overlap. For most of the cases, the number spectra in this size range are similar for Hiac and Coulter. This may be an indirect indication that the sample manipulation for Hiac processing provides minimal bias. The final HIAC data for a given sample was calculated by averaging results from four 25 ml replicate measurements.

Larger particles ($d > 60 \mu\text{m}$) were enumerated in situ using the UVP. Two cameras of 732×570 pixel resolution and 12 Hz of frequency with different zoom lenses (25 and 8 mm) were positioned perpendicularly to an 8 cm thick light beam generated by two 54 W Chadwick Helmuth stroboscopes and took their images simultaneously. Only particles illuminated against a dark background were observable. The volumes sampled were 1.25 and 10.5 L for the high and low magnification cameras. The short flash duration (pulse duration = 30 μs) allowed a fast lowering speed (up to 1.5 m/s) without deterioration of image quality. The images of the UVP were analyzed after the deployment by custom-made software on a laboratory computer (Gorsky et al., 2000). Objects in each image were detected, sized and enumerated. The measurement is based on the lateral scattering of light from a particle; the instrument reports the particle size as a total number of pixels, which is converted to ESD. The UVP recorded images over the entire depth range that it was lowered, with one image acquired every 8 cm. In order to avoid contamination of the images by solar light, we have only used images obtained deeper than 40 m for day profiles.

We averaged UVP data collected within 2.5 m of the sampled depth to compare with samples collected with the Niskin sampler. Thus, the sampled volumes were effectively 100 ml, 75 L and 630 L for the HIAC and UVP (small and large zoom cameras) respectively in the Marquesas station. In the Gyre the UVP data were combined within 5 m of the depth because of the lower particle concentrations there, yielding sample volumes of 150 and 1260 L for the UVP cameras.

2.3 Calculating the number and mass size spectra

The particle size spectrum (n , particle number $\text{cm}^{-3} \text{cm}^{-1}$) is a useful description of the relationship between particle abundance and size. This relationship generally follows a power law function of the form:

$$n = bd^{-k} \quad (1)$$

where b is a constant, k the slope and d the particle diameter (Sheldon et al., 1972). The number spectrum, $n = dN/dd$, can be calculated from dN , the total number of particles per unit volume in a diameter range between d and $d+dd$ where dd is a small diameter increment.

Different instruments measure different particle properties and, hence, can give different estimates of particle diameter. For example, the Coulter Counter measures the change in electrical resistance when a particle passes through an orifice. The resistance is approximately proportional to the solid particle volume (the *conserved volume*) and excludes any water between the solid parts of an aggregate. The diameter of a sphere with that volume is the *conserved diameter*, d_c ; The diameter of the overall object, including any contained water is the *fractal diameter*, d_f . The two are related using fractal scaling (Jackson, 1990). For a solid object the two diameters are the same but they can be very different if the particle is porous, as marine aggregates are.

When we combine the data from the two instruments, we will discuss the possibility that the HIAC reports a conserved diameter and the UVP a fractal diameter. To convert between a number spectrum calculated using d_f (n_f) and one calculated using d_c (n_c) we use the following equation:

$$n_c = n_f \frac{dd_f}{dd_c} \quad (2)$$

The conversion of n_f to n_c requires a relationship between particle fractal diameter and conserved diameter. Fractal scaling provides such a relationship. The two key descriptors are an initial cell diameter d_1 and a fractal dimension for aggregates D_3 and the underlying hypothesis are that all aggregates are formed from the aggregation of a single type of particles (phytoplankton cells) and that the porosity of the aggregates is constant on the entire size spectra. To simplify the complexity of the natural assemblage of phytoplankton cells during the cruise, we assumed values of $d_1 = 5 \mu\text{m}$ because the nanophytoplankton were present at both sites. We have tested three different values of the fractal dimension (1.9, 2.3 and 3) for the conversion. The two first values have been estimated as being the minimum and average values obtained by comparing 118 UVP size spectra data obtained in different cruises with combined measured vertical flux in sediment traps using a Monte Carlo procedure (Guidi et al., 2008). This data set used to constrain the aggregate fractal dimension contains the sediment traps data of the BIOSOPE cruise. Using the vertical flux of particles to constrain the UVP size spectra is more accurate than using POC data because the

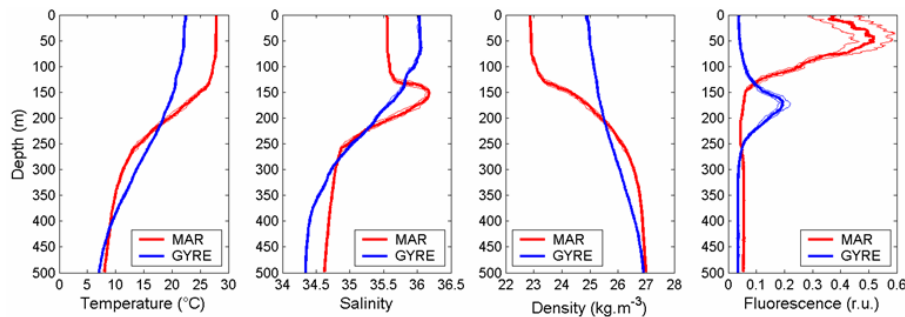


Fig. 2. Median, first quartile and third quartile of all verticals profiles of the CTD data at the MAR ($n=29$) and GYR sites ($n=35$). The hydrological parameters were (from left to right): temperature ($^{\circ}\text{C}$), salinity, density ($\text{kg}\cdot\text{m}^{-3}$) and fluorescence (relative unit).

main vectors of flux are the large settling aggregates. These fractal dimensions are within the range of previous estimates, which range from 1.3 to 2.49 (Jackson et al., 1997; Kilps et al., 1994; Li and Logan, 1995; Logan and Wilkinson, 1990; Xiaoyan and Logan, 1995). The value of 3 is the upper limit and occurs when porosity is constant with diameter. The conserved volume distribution can be calculated from n_c assuming a sphere. The total mass can be calculated knowing the density of the matter in the sphere. At all sites and depth, we use a constant cell density ($\rho=1.027\text{ g cm}^{-3}$) to estimate the total particle mass M .

$$M = \int_0^{\infty} n_c \rho \frac{4\pi}{3} \left(\frac{d_c}{2}\right)^3 dd_c \quad (3)$$

These values of dry weight (DW) can be converted to POC assuming POC=50% DW (Stramski et al., 2008; Alldredge, 1998) and compared to independent POC measurements. The samples for POC analysis were collected on precombusted (450°C) GF/F filters (25 mm in diameter) on board R/V l'Atalante. For each station at all sites, two depth layers were examined in two or three replicated samples. Volume of filtered seawater varied from 0.7 to 8.4 L depending on the station and the concentration of particulate matter in the water (Stramski et al., 2008).

2.4 Size range

The particle size spectra can be calculated by dividing the particle size range into sub-ranges called bins. The HIAC instrument has 50 bins having a log-normal size progression between 1.5 and 100 μm while the UVP data process used for the BIOSOPE cruise has 27 bins having a log-normal size progression between 60 and 5000 μm . In the following, the particles ($<30\text{ }\mu\text{m}$) detected by the HIAC instrument will be referred as small particles while the particles ($>100\text{ }\mu\text{m}$) detected by the UVP will be referred as large particles. Number spectra with respect to the reported diameters were calculated by dividing the number concentration of particles in a section by the section width.

Both the HIAC and UVP techniques undersample particles at the lower end of their size ranges, producing anomalous peaks in size spectra. Therefore, we considered only the part of the spectra after the peaks. At the upper limit of the size range for any instrument, there are too few particles are present in a section to allow reliable estimates of particle concentrations, resulting in poor sampling statistics. Assuming that the number of particles within a section is described by a Poisson distribution, there is a counting error estimated as the square root of the mean number of particles in that section (Jackson et al., 2005). We excluded values with 4 or fewer particles within a section from our analysis to exclude counts with too high an uncertainty. As a result, the effective size ranges of both instruments were lower than the nominal size ranges; typically 3.5–30 μm for the HIAC (instead of 1.7–100 μm) and 100–2000 μm for the UVP (instead of 60 μm –5000 μm). Note that the actual upper size limits of both instruments varied slightly as a function of the actual particles abundances. The slopes of the size spectra ($-k$) were calculated independently for the HIAC and UVP with values at either end of their size ranges excluded. In the following, the particles ($<30\text{ }\mu\text{m}$) detected by the HIAC instrument will be referred as small particles while the particles ($>100\text{ }\mu\text{m}$) detected by the UVP will be referred as large particles.

3 Results

3.1 Hydrography and biogeochemistry of the two sites (MAR and GYR)

In the MAR stations, surface waters were warm (up to 27°C) and relatively fresh (~ 35.6) (Fig. 2). The surface layer had a relatively constant temperature to 70–100 m depth. A subsurface fluorescence maximum developed at $\sim 60\text{ m}$ in the mixed layer and corresponded to a measured maximum of $0.38\text{ mg Chl-}a\text{ m}^{-3}$ in the water bottle data (Table 1). There was greater salinity deeper than 100 m signifying the presence of more saline South Tropical Water (the maximum at

Table 1. Properties of the MAR and GYR sites.

| | MAR | GYR |
|---|-----------------|------------------|
| 0–200 m integrated chlorophyll- <i>a</i> (mg m^{-2}) | 32.6 ± 2.72 | 20.56 ± 1.17 |
| Maximum chlorophyll- <i>a</i> (mg m^{-3}) | 0.38 ± 0.05 | 0.17 ± 0.008 |
| Maximum chlorophyll- <i>a</i> depth | 55 ± 14 m | 176 ± 9 m |
| Euphotic zone depth (<i>Ze</i>) | 72 ± 5 m | 160 ± 4 m |
| Mixed layer depth | 85 ± 9 m | 40 ± 31 m |

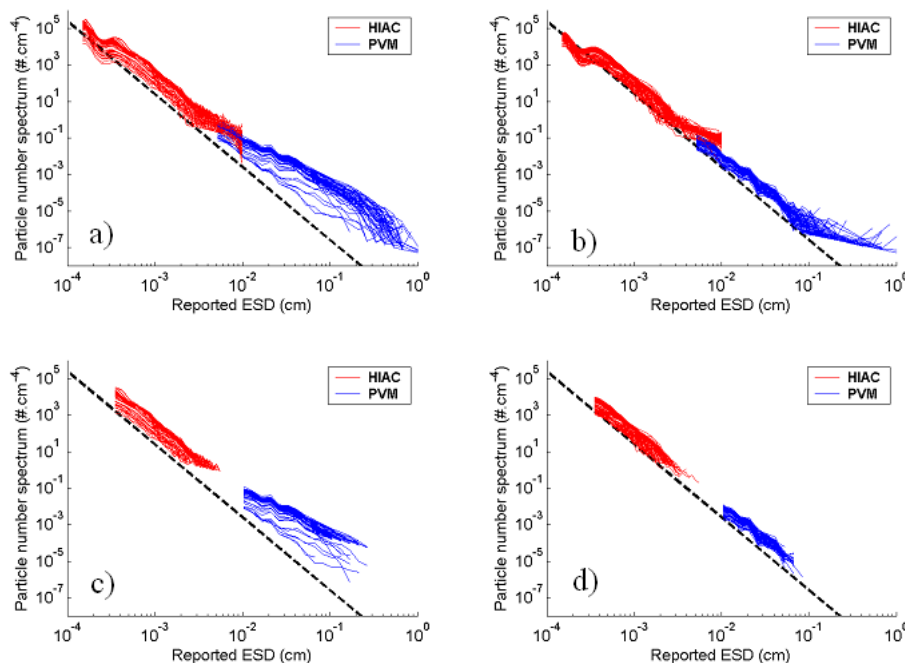


Fig. 3. All number spectra in the upper 200 m depth from the HIAC (red) and the UVP (blue) at the MAR site (a and c) and GYR site (b and d). (a) and (b) are the raw spectra while (c) and (d) are the lower and larger end truncated spectra to account for methodological biases. The slopes of the number spectra have been calculated using (c) and (d). These spectra were calculated using the particle diameters reported by the different instruments. The dashed reference line has a slope of -4 .

160 m). The mean depth of the euphotic zone in this region was 72 m.

The GYR stations differed by having higher surface salinity and lower surface temperature than MAR. The mixed layer was more poorly delimited than at the MAR stations. The GYR stations had extremely low levels of Chl-*a* fluorescence in the surface layer and a Deep Chlorophyll Maxima (DCM), $\sim 0.16 \text{ mg Chl-}a \text{ m}^{-3}$ at around 170 m depth. The mean depth of the euphotic zone in this region was 160 m (Table 1). The TS distributions were relatively constant at both MAR and GYR over the sampling period. The complete description of each site can be found in (Claustre et al., 2008).

3.2 Typical size spectra at GYR and MAR

The number spectra from both instruments at both sites followed the standard pattern of decrease in abundance with increasing reported diameter (Fig. 3). Raw spectra from both instruments show the typical biases at either end of their size ranges. The data follow a nearly straight line at GYR but not at MAR. In this latter site, the slope is not as steep in the size range covered by the UVP.

3.3 Distribution of particle concentrations and spectral slopes at the GYR site

The two instruments showed different vertical patterns for the two populations of particles (Fig. 4). The small particles detected by the HIAC showed higher concentrations in

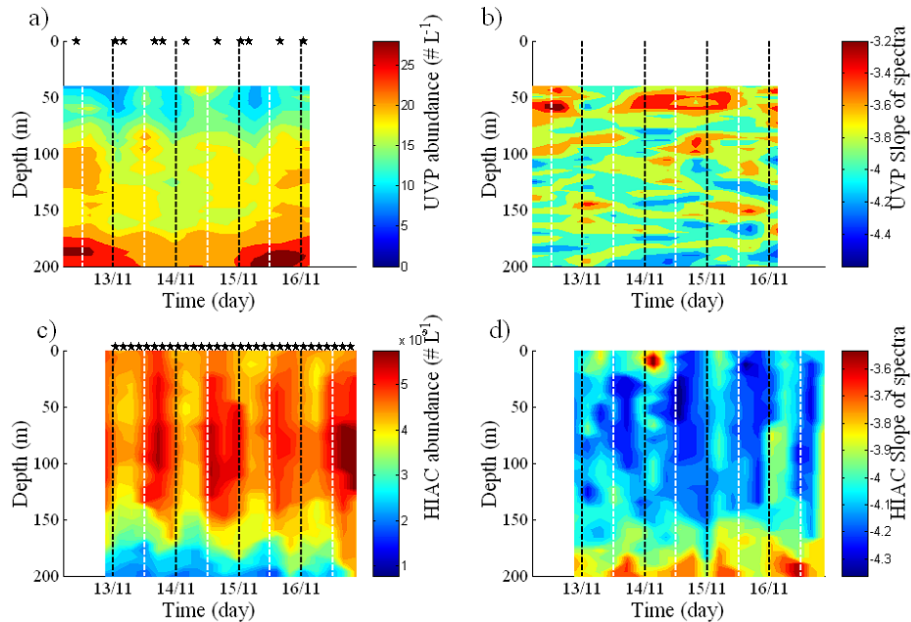


Fig. 4. Temporal distribution of the total particle abundance at the GYR site of the UVP (a) and HIAC (c) and particle slope of size spectra of the UVP (b) and HIAC (d). The black dashed lines indicate local mid-night time while the white dashed lines indicate local mid-day time. The sampling is indicated by the stars.

the upper 150 m with maxima at 100 m. In addition, they showed a strong diel cycle. The maximum of particle abundance occurred in the afternoon, around 4:30 p.m. Note that the attenuation coefficient at 660 nm, a proxy of the carbon concentration, presents exactly the same pattern of diel variation (Claustre et al., 2007a). These diel cycles were coupled with a diel cycle in the slopes of the size spectra. The average slopes over the HIAC size range were steeper during the afternoon around 4:30 p.m. and flatter during the night. The large particle concentrations estimated with the UVP were highest below 100 m depth. The diel variations observed for the small particle slopes were not detectable for the large particles in the UVP data below 40 m.

3.4 Distributions of particle concentrations and spectral slopes at the MAR site

Both large and small particle concentrations were greatest in the upper 80 m at MAR (Fig. 5). Small particles in the upper 75 m had diel cycles for concentration and slope. The pattern of this cycle was identical to that was observed at the GYR station. The large particles detected by the UVP did not show such diel cycles but there was a decrease in abundance and spectral slope after 28 October. The minimum slope was at 100 m depth on 27 October, but was at 140 m depth on 29 October. Note that the temporal decrease of large particles was accompanied by a decrease of the small particles. The spectral slopes of the large particles were lower ($2.3 < kP < 2.5$) than those for the small particles ($3.9 < k < 3.7$) in the upper 200 m depth.

3.5 Frequency distributions of spectral slope

The spectral slope values for HIAC particles averaged about 4 during the day and 3.9 during the night at MAR (Fig. 6). At GYR, the small particles showed a double peak for the slope at day (3.95 and 3.7) and one peak at night (3.7). The slopes of 3.7 at day were from deeper than 150 m depth while those with a value of 3.95 were in the upper 100 m (see Fig. 4d). In contrast two distinct slope modes and no diel variation were observed for the large particles detected by the UVP, at values centered on 3.8 and 2.5, respectively for the GYR and MAR sites.

4 Discussion

4.1 Potential origin of particles

Neither the HIAC nor the UVP differentiated between living organisms and detrital material. Additional information collected during the cruise, including WP2 0–200 m vertical net samples (for mesozooplankton counted with the ZOOSCAN system (Grosjean et al., 2004)), microscopic counts of water samples, pigment characterization by HPLC and in situ optical properties, can provide insight to the nature of the particle making up the size spectra.

At GYR, the peak of small particles centered at 100 m was not associated with a peak of fluorescence although it corresponded to a peak of *Prochlorococcus* and a population of non vegetal particles (Grob et al., 2007). According to Grob et al. (2007), the proportion of vegetal particles

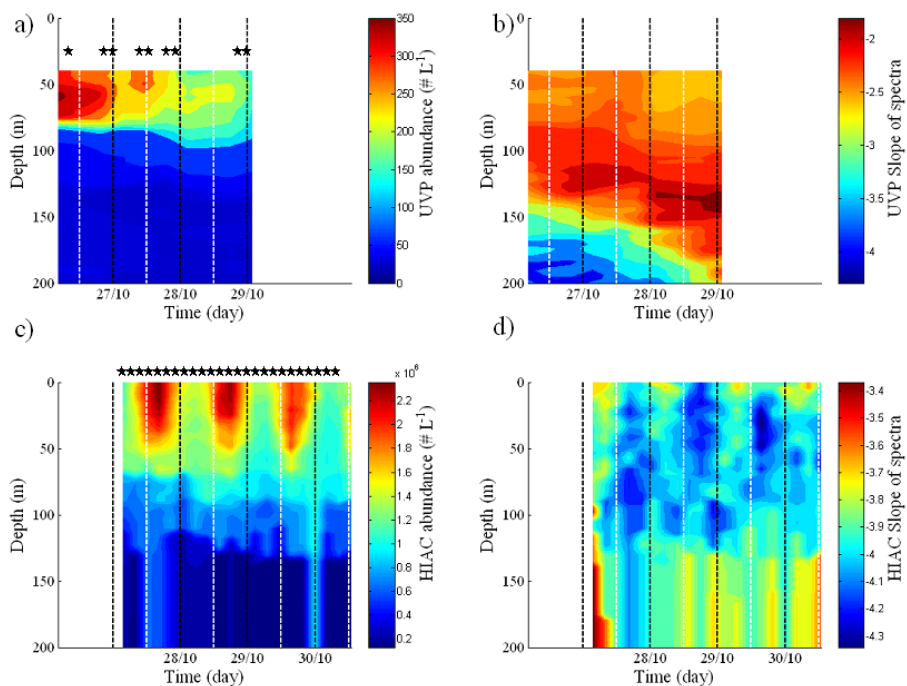


Fig. 5. Temporal distribution of the total particle abundance in the MAR site of the UVP (a) and HIAC (c) and particle slope of size spectra of the UVP (b) and HIAC (d). The black dashed lines indicate local mid-night time while the white dashed lines indicate local mid-day time. The sampling is indicated by the stars.

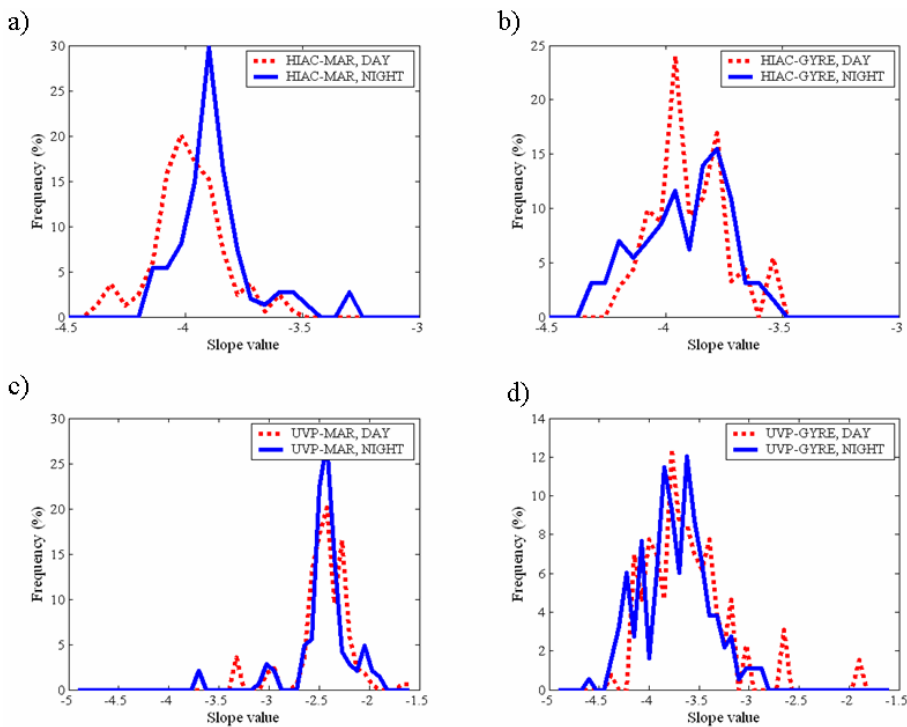


Fig. 6. Day and night frequency distribution of the spectral slopes for particle distributions determined by the HIAC (a) for MAR and (b) for GYR) and the UVP (c) for MAR and d) for GYR).

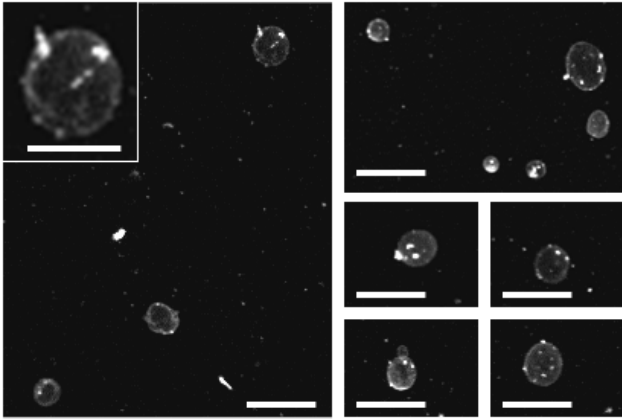


Fig. 7. UVP video images of the unidentified large objects at MAR. All the scale bars are 5 mm but the one in the upper left corner where it is 3 mm.

increased with depth and was the highest in the DCM. Algae in the DCM were mainly picophytoeukaryotes, although some coccolithophorid plates and diatom cells were also present (Beaufort et al., 2007; Gómez et al., 2007; Ras et al., 2007). The small particle did not show any peak in the DCM probably because the minimum size used to calculate the size spectra (3.5 μm) is larger than the dominant phytoplanktonic cells. The large particles had only one maximum in the DCM that was found in all profiles suggesting that the particles at 100 m depth were not a source of aggregates but that the active picophytoeukaryotes, coccolithophorid plates and diatom cells found in the DCM could be. The aggregates that form the material observed by the UVP could also be detritus produced by zooplankton because the Phaeophorbide pigment (a tracer for altered Chl-*a* found in faecal pellets) concentration also had a maximum in this layer (Ras et al., 2007). The large particles could not have been living mesozooplankton ($d > 200 \mu\text{m}$) because animal concentrations in the upper 200 m depth averaged less than 0.1 ind. L^{-1} (personal data) compared to the large particles estimates of 20 part. L^{-1} . In the MAR site, concentration of microphytoplankton ($10 < d < 100 \mu\text{m}$, mostly small pennate diatoms of the genus *Pseudonitzschia*) ranged from 1000 to 32 000 cells L^{-1} (Gómez unpublished data). These concentrations are in the same range as the HIAC counts for particles $d > 10 \mu\text{m}$ (5500 \pm 250 cells L^{-1}). Therefore, many of the particles larger than 10 μm detected by the HIAC in the MAR site were probably diatom cells. Aggregates of *Pseudonitzschia delicatissima* and large *Rhizosolenia bergonii* were observed from 50 to 100 m depth with concentrations of 2 to 20 aggregates L^{-1} and constituted some of the particles larger than $d > 100 \mu\text{m}$. Again, mesozooplankton were not an important fraction of the large particles because their concentrations in the upper 200 m layer were less than 1 ind. L^{-1} (personal data), compared to UVP particle concentrations as great as 100 part L^{-1} .

Most of the large object detected in the UVP images at MAR site were transparent disk-shaped objects with $d = 2\text{--}5 \text{ mm}$ present at concentrations of 1–10 L^{-1} (Fig. 7). They were located throughout the upper 200 m but had a maximum concentration between 120 and 170 m depth. These objects had different shapes than single celled or aggregated large diatoms such as the abundant *Rhizosolenia bergonii* and were not observed in the visual count of samples from Niskin bottles or plankton nets possibly because they had been destroyed during the sample processing. Their shapes are similar to those of large dinoflagellates, such as *Noctiluca*, but these objects are larger. They have not yet been identified but seem to be living organisms. They are mostly responsible for the smaller spectral slopes and the large calculated particle biomass at the MAR site deeper than 100 m. Their role and importance in the ecosystem remain unknown.

4.2 Uncoupled temporal dynamics of small and large particle pools

Small particles showed clear diel cycles in both total abundance and relative size distribution at both MAR and GYR that were not observed in particles detected by the UVP. At a first view, the variations in particle concentration (Figs. 4 and 5) and mean size (data not shown) do not support a phenomenon of autotrophic division where size normally increases during the day due to C fixation, and particle number increases at night due to cell division, although the variation of attenuation coefficient measured at the GYR and MAR stations clearly support diel cycle of C fixation (Claustre et al., 2008). In fact, the variations of particle abundance and size measured within a given size interval are difficult to interpret because they do not necessarily concern the same pools of particles. The unexpected increase of particle concentration observed during the day may correspond to the arrival in the interval of measurement of smaller growing particles, and not only to the division of particles belonging to this size range. This hypothesis is supported by the variations of the slope values which are steeper in the afternoon. The counts acquired with the Coulter counter in the range 0.7–5 μm clearly shows that diel variations of particle number and size obey to a process of cell divisions of picoeucaryotes (Sciandra, personal communication).

These diel variations were not observed in particles detected by the UVP. The fact that this pattern of variability was not observed for the pool of large particles suggests that the dynamics of small and large particles are disconnected at the diel scale. Diel cycles in the large particle spectra do occur (Graham et al., 2000; Lampitt et al., 1993; Stemmann et al., 2000). Explanations that have been proposed to explain them include the disaggregation (Dilling and Alldredge, 2000) or the fecal pellet production (Stemmann et al., 2000) by zooplankton engaged in their daily vertical migration and the periodic coagulation driven by diel cycles in turbulence (Ruiz, 1997). The diel change in the small particle pool is due to

cell division rather than diel biomass growth. The observation that they are uncoupled during the cruise suggests that this life cycle pattern of the phytoplankton cell does not lead to the formation of aggregates because processes in algae are not sufficient to move mass from the primary cells to larger aggregates for these short time scales and low particle concentrations. The diel vertical migration of total zooplankton was not observed in the net data and therefore could not affect the size spectra of the UVP particles.

4.3 Combining the HIAC and UVP size spectra

Care must be taken when comparing results from different instruments because they may not measure the same particle properties. Even the diameter reported by a single instrument can vary depending on the nature of the object (single cell versus aggregate). For example, aperture impedance particle counters, such as the Coulter Counter, measure a particle property that corresponds approximately to the volume of the solid mass composing a porous particle, while imaging instruments frequently measure the cross sectional area of the porous aggregate (Jackson et al., 1997).

The operational size range for the UVP is dominated by porous aggregates ($>60\ \mu\text{m}$). For this reason, it was calibrated with a variety of aggregates whose cross-sectional areas were determined using a stereo microscope. We denote the diameter reported by the UVP as a “fractal diameter”, d_f , because it is not proportional to a mass-equivalent spherical diameter but similar to the outer diameter of a fractal particle. In contrast, the HIAC works in a size range where there are solid single cells ($<20\ \mu\text{m}$) as well as porous aggregates ($>20\ \mu\text{m}$). Laboratory experiments performed on monospecific phytoplankton cultures have shown good agreement between mono-dispersed size distributions measured with HIAC and Coulter particle counters, although the diameters reported by the HIAC can be as much as 10% smaller than those from the Coulter counter. Multiple measurements made on different phytoplankton cultures with the HIAC showed very good agreement between the biovolume calculated assuming that the algae are spheres with the reported diameters and the particulate carbon concentration measured separately, suggesting that the light blockage is proportional to the mass content of the algae. Therefore, we consider the particle diameter reported by the HIAC to be an estimate of the “conserved” diameter, d_c .

However, the assumption that the HIAC reports a conserved diameter may not hold in the case of small aggregates for which the instrument could be respond to the fractal diameter. If we assume that the reported diameter is a fractal diameter and that $D_3=2.3$ then the number spectrum is shifted toward the small particle size compared to the case where d is a conserved diameter (Fig. 8). The explanation is that for a plain sphere, $d_c=d_f$ while for a porous sphere d_f is larger than d_c . As a result, the number spectrum is shifted toward larger size when $d=d_c$. Accordingly, there is

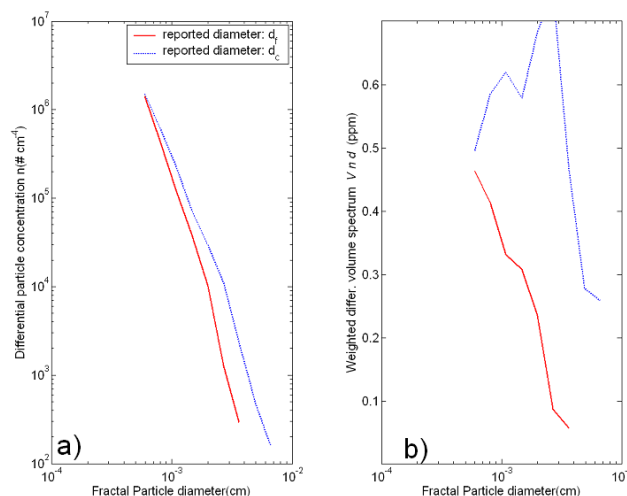


Fig. 8. (a) Number and (b) mass spectra calculated assuming that the HIAC reports a fractal diameter (d_f) and $D_3=2.3$ or a conserved diameter (d_c). The spectrum used in this figure was calculated as the median spectrum of all the samples at the GYR site.

more mass in solid sphere than in porous one of the same diameter and the mass spectrum shows an increase in mass when expressed in terms of d_c . The total HIAC mass is on average 2 times higher if we assume that $d=d_c$. Therefore, this assumption yields a maximum estimate of the total mass contained in the small particles.

We can calculate the mass distribution and a maximum estimate of the total volume of the aggregates using Eq. (3) and assuming that the HIAC reports a conserved diameter and that the UVP reports a fractal diameter. We will assume three fractal dimensions, 1.9, 2.3 and 3. Despite the relative straight nature of the number spectra when plotted using log-log axes, the mass spectra show greater variability because small deviations from the straight line induce large variations in the mass estimates. Therefore, the slope cannot be used to determine the mass distribution of marine particles although it can be a synthetic descriptor of the system. At the GYR site, the volume spectra of particles varied from a dominance of particles smaller than $100\ \mu\text{m}$ ($D_3=1.9$ and 2.3) to a dominance of larger particles ($D_3=3$) (Fig. 9). At the MAR site, the volume of the UVP particle in each bin is always much larger than the HIAC particles volume. The biovolume calculated using the different fractal dimensions varies by a factor of up to 20 showing the sensitivity of estimating the mass using particle size spectra.

The total mass of the HIAC particles should be similar to the total mass obtained from GF/F filtration but not the UVP particles because the sampling volume for the GFF filtration was too low to sample the large particles adequately. The HIAC POC estimates assuming that the HIAC reports a conserved diameter were higher than those measured independently by a factor of two. If we assume that the HIAC

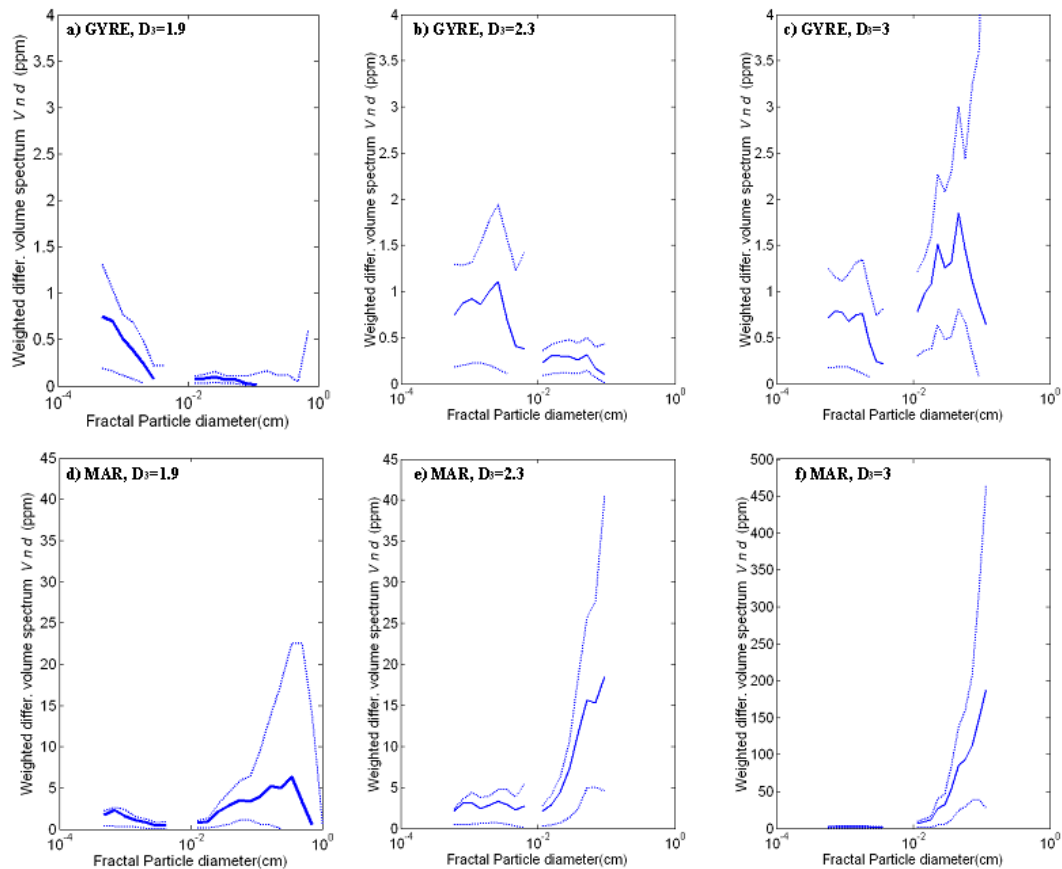


Fig. 9. Percentiles (5%, 50% and 95 %) of each size bin of the particle mass spectra for samples at the GYR site (**a**, **b** and **c** $n=87$) and MAR site (**d**, **e** and **f**, $n=85$). The 5 and 95 percentiles represent the envelope of the observed mass spectra. The area under a curve is the total particle solid volume concentration. The mass of large particles has been calculated using two values for the fractal dimension 1.9 (left column), 2.3 (centre column) and 3 (right column).

reports a fractal diameter, then the POC estimates are of the same range than those measured at 150 m depth with the lowest fractal dimension of 1.9 (Fig. 10). At 5 m, the biomass spectra always exceed the POC estimates. The changes with depth and also sites of the ratio between calculated and measured POC concentrations could also reflect change in the particle properties (higher porosity at surface for instance) that the model does not take into account because of the lack of information on particle properties. The mass dominance of the UVP particles at MAR site may be a methodological artefact because the basic hypothesis of a single relationship between particle mass and diameter is invalid. In that site, we observed a great number of large living objects with probably a lower volume to mass ratio than that of equal-diameter aggregates. This discrepancy highlights the need for a correct estimation of the particle properties when converting the particle size reported by any instrument to the particle mass, particularly if the particles are in fact aggregates for which the fractal and conserved diameter are not the same. Many reports assume that the particles are solid, implying $D_3=3$,

and probably overestimate the importance of the large particles in the mass distribution.

If we extend the mass spectra calculation (with $D_3=1.9$ and 2.3) to all the profiles with combined spectra collected during the cruise then we can estimate the importance of the two populations of particles across the upper 300 m depth of the South Pacific Gyre (Fig. 10). The mass concentrations of both particle populations decreased from the mesotrophic site of the HNLC to the ultraoligotrophic GYR following the trophic trend observed for phytoplankton and c_p (Ras et al., 2007; Grob et al., 2007). We can estimate that the proportion of mass contained in the large particles decreased from the mesotrophic conditions at the border of SPG to the ultraoligotrophy of GYR. However, at GYR site, the disproportion of mass between the two particle pool decreased with depth and using a $D_3=2.3$, the larger fraction equated the mass of the small particles deeper than 200 m depth (data not shown). Therefore, we expect large particles to play an equal or major role in the trophic interaction in the upper waters of the South Pacific Gyre.

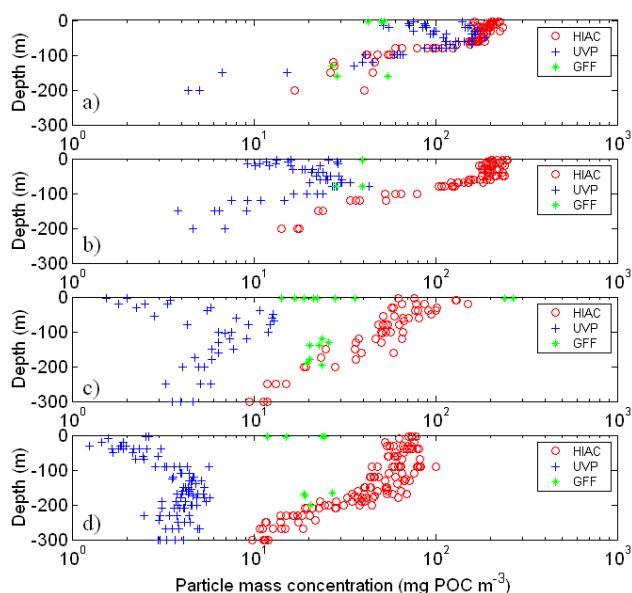


Fig. 10. Vertical profiles of particle mass for the HIAC and the UVP (with $D_3=1.9$ and assuming that both instruments report a fractal diameter) and GF/F POC content in the four sites investigated during the first leg of the BIOSOPE cruise, (a) MAR, (b) HNLC, (c) STA and (d) GYR. The same estimates were made using $D_3=2.3$ but the figures are not shown.

5 Conclusions

The particle size distribution from few μm to few mm cannot always be fit with a unique power relationship. At MAR, the high abundance of large probably living organisms created a shift in the full size spectra of particles. The small ($<30 \mu\text{m}$) and large ($>100 \mu\text{m}$) particle pools have different diel patterns. This implies that the exchange of mass toward the large particles does not take place at daily scale in the SPG area.

Care must be taken when comparing size spectra using different instruments that may not measure the same particle property. Knowing the geometric properties of the particles is crucial to calculate the mass from the particle size spectra because the mass estimates can change by several orders of magnitudes using different parameters to describe aggregates porosity. We show using consistent values to describe particle properties that the number spectra can provide realistic estimates of particle mass for regions where the particle population is composed of particles and aggregates. Using a fractal dimension of 1.9 and 2.3 to describe the porosity of the large aggregates, we calculated the total mass in the different regions of the SPG. Results show that the mass of large particles ($>100 \mu\text{m}$) can equal the mass in the smaller particles. Overall this study highlights the need for measures of particle properties to be able to use the size spectra in biogeochemical applications.

Acknowledgements. This work was supported by the French program PROOF (Processus Biogéochimiques dans l’Océan et Flux), Centre National de la Recherche Scientifique (CNRS), the Institut des Sciences de l’Univers (INSU) and the ZOOPNEC program, part of the French framework of the PNEC project. GJ’s contribution was supported by NSF grants OCE-0352127 and OCE-0327644. L. Guidi was financially supported by Ministère de la l’Education et de la Recherche and CNRS (France). We also thank the scientific party and the Captain and crew of the RV L’Atalante during the BIOSOPE Expedition and D. Stramski, M. Babin, C. Crob and M. Twardowski who have contributed to the HIAC and POC measurements. We also thank the three reviewers for their useful comments.

Edited by: M. Dai

References

- Allredge, A.: The carbon, nitrogen and mass content of marine snow as a function of aggregate size, *Deep Sea Res. I*, 45, 529–541, 1998.
- Beaufort, L., Couapel, M., Buchet, N., and Claustre, H.: Calcite production by Coccolithophores in the South East Pacific Ocean: from desert to jungle, *Biogeosciences Discuss.*, 4, 3267–3299, 2007, <http://www.biogeosciences-discuss.net/4/3267/2007/>.
- Claustre, H., Huot, Y., Obernosterer, I., Gentili, B., Tailliez, D., and Lewis, M.: Gross community production and metabolic balance in the South Pacific Gyre, using a non intrusive bio-optical method, *Biogeosciences Discuss.*, 4, 3089–3121, 2007, <http://www.biogeosciences-discuss.net/4/3089/2007/>.
- Claustre, H., Sciandra, A., and Vaultot, D.: Introduction to the special section Bio-optical and biogeochemical conditions in the South East Pacific in late 2004: the BIOSOPE program, *Biogeosciences Discuss.*, 5, 605–640, 2008, <http://www.biogeosciences-discuss.net/5/605/2008/>.
- Dilling, L. and Allredge, A. L.: Fragmentation of marine snow by swimming macrozooplankton: A new process impacting carbon cycling in the sea, *Deep Sea Res. I*, 47, 1227–1245, 2000.
- Gómez, F., Claustre, H., Raimbault, P., and Souissi, S.: Two High-Nutrient Low-Chlorophyll phytoplankton assemblages: the tropical central Pacific and the offshore Per-Chile Current, *Biogeosciences*, 4, 1101–1113, 2007, <http://www.biogeosciences.net/4/1101/2007/>.
- Gorsky, G., Picheral, M., and Stemann, L.: Use of the underwater video profiler for the study of aggregate dynamics in the north Mediterranean, *Estuar. Coast. Shelf S.*, 50, 121–128, 2000.
- Graham, W. M., MacIntyre, S., and Allredge, A. L.: Diel variations of marine snow concentration in surface waters and implications for particle flux in the sea, *Deep-Sea Res. I*, 47, 367–395, 2000.
- Grob, C., Ulloa, O., Claustre, H., Huot, Y., Alarcón, G., and Marie, D.: Contribution of picoplankton to the total particulate organic carbon concentration in the eastern South Pacific, *Biogeosciences*, 4, 837–852, 2007, <http://www.biogeosciences.net/4/837/2007/>.
- Grosjean, P., Picheral, M., Warembourg, C., and Gorsky, G.: Enumeration, measurement, and identification of net zooplankton

- samples using the zooscan digital imaging system, *ICES J. Mar. Sci.*, 61, 518–525, 2004.
- Guidi, L., Gorsky, G., Claustre, H., Picheral, M., and Stemmann, L.: Contrasting distribution of aggregates $>100\ \mu\text{m}$ in the upper kilometre of the South-Eastern Pacific, *Biogeosciences Discuss.*, 5, 871–901, 2008, <http://www.biogeosciences-discuss.net/5/871/2008/>.
- Jackson, G. A.: A model for the formation of marine algal flocs by physical coagulation processes, *Deep-Sea Res. I*, 37, 1197–1211, 1990.
- Jackson, G. A., Logan, B. E., Alldredge, A. L., and Dam, H. G.: Combining particle size spectra from a mesocosm experiment measured using photographic and aperture impedence (coulter and elzone) techniques, *Deep-Sea Res. II*, 42, 139–157, 1995.
- Jackson, G. A., Maffione, R., Costello, D. K., Alldredge, A., Logan, B. E., and Dam, H. G.: Particle size spectra between $1\ \mu\text{m}$ and $1\ \text{cm}$ at monterey bay determined using multiple instruments, *Deep Sea Res. I*, 44, 1739–1767, 1997.
- Jackson, G. A., Waite, A. M., and Boyd, P. W.: Role of algal aggregation in vertical carbon export during soiree and in other low biomass environments, *Geophys. Res. Lett.*, 32, L13607, doi:13610.11029/12005GL023180, 2005.
- Kilps, J. R., Logan, B. E., and Alldredge, A. L.: Fractal dimensions of marine snow determined from image analysis of in situ photographs, *Deep Sea Res. I*, 41, 1159–1169, 1994.
- Lampitt, R. S., Hillier, W. R., and Challenor, P. G.: Seasonal and diel variation in the open ocean concentration of marine snow aggregates, *Nature*, 362, 737–739, 1993.
- Li, X. and Logan, B. E.: Size distributions and fractal properties of particles during a simulated phytoplankton bloom in a mesocosm, *Deep-Sea Res. II*, 42, 125–138, 1995.
- Logan, B. E. and Wilkinson, D. B.: Fractal geometry of marine snow and other biological aggregates, *Limnol. Oceanogr.*, 35, 130–136, 1990.
- Mikkelsen, O. A., Milligan, T. G., Hill, P. S., and Moffatt, D.: Insect – an instrumented platform for investigating floc properties close to the seabed, *Limnol. Oceanogr.-Methods*, 2, 226–236, 2004.
- Ras, J., Claustre, H., and Uitz, J.: Spatial variability of phytoplankton pigment distributions in the Subtropical South Pacific Ocean: comparison between in situ and predicted data, *Biogeosciences Discuss.*, 4, 3409–3451, 2007, <http://www.biogeosciences-discuss.net/4/3409/2007/>.
- Ruiz, J.: What generates daily cycles of marine snow?, *Deep-Sea Res. I*, 44, 1105–1126, 1997.
- Sheldon, R. W. and Kerr, S. R.: The population density of monsters in loch ness, *Limnol. Oceanogr.*, 17, 796–798, 1972.
- Sheldon, R. W., Prakash, A., and Sutcliffe Jr., W. H.: The size distribution of particles in the ocean, *Limnol. Oceanogr.*, 17, 327–340, 1972.
- Stemmann, L., Picheral, M., and Gorsky, G.: Diel variation in the vertical distribution of particulate matter ($>0.15\ \text{mm}$) in the nw mediterranean sea investigated with the underwater video profiler, *Deep Sea Res. I*, 47, 505–531, 2000.
- Stramski, D., Reynolds, R. A., Babin, M., Kaczmarek, S., Lewis, M. R., Röttgers, R., Sciandra, A., Stramska, M., Twardowski, M. S., Franz, B. A., and Claustre, H.: Relationships between the surface concentration of particulate organic carbon and optical properties in the eastern South Pacific and eastern Atlantic Oceans, *Biogeosciences*, 5, 171–201, 2008, <http://www.biogeosciences.net/5/171/2008/>.
- Xiaoyan, L. and Logan, B. E.: Size distributions and fractal properties of particles during a simulated phytoplankton bloom in a mesocosm, *Deep-Sea Res. II*, 42, 125–138, 1995.